

Journal of Molecular Science

Biosorption and Metal Tolerance Capabilities of *Bacillus subtilis*: Implications for Bioremediation

SN Praveena Yadavalli¹, Sreenivasulu Kamma², Debasish Sahoo^{*3}

¹Ph.D Scholar, Department of Biotechnology, KL University Vaddeswaram, Andhra Pradesh, India
ORCID- 0000-0001-7246-3854

²Department of Biotechnology, KL University Vaddeswaram, Andhra Pradesh, India

³*BioInnovale Lifescience Pvt. Ltd. Bengaluru, India

Article Information

Received: 13-10-2025

Revised: 06-11-2025

Accepted: 26-11-2025

Published: 23-12-2025

Keywords

Bacillus subtilis, Biosorption, Heavy Metal, Nitrogen, Chromium, FTIR.

ABSTRACT

Bacillus subtilis, a widely studied bacterium, demonstrates remarkable tolerance to heavy metals and significant biosorption capacity, offering potential applications in bioremediation. This study evaluates the resistance mechanisms of *B. subtilis* to various metals, including lead, zinc, arsenic and chromium, and examines its ability to absorb these contaminants from aqueous solutions with optimization of the carbon and nitrogen source. Results reveal that cell wall components and exopolysaccharides play a crucial role in metal binding. Optimization of environmental conditions enhances biosorption efficiency, showcasing the adaptability of *B. subtilis*. The findings underscore its utility as a cost-effective, eco-friendly solution for mitigating heavy metal pollution in industrial wastewater and contaminated environments.

©2025 The authors

This is an Open Access article distributed under the terms of the Creative Commons Attribution (CC BY NC), which permits unrestricted use, distribution, and reproduction in any medium, as long as the original authors and source are cited. No permission is required from the authors or the publishers. (<https://creativecommons.org/licenses/by-nc/4.0/>)

levels (Pham et al., 2022). Heavy metal exposure, such as lead, mercury, and cadmium, can cause major health problems in humans, including neurological abnormalities, renal damage, and developmental disabilities (Pagliaccia et al., 2022; Ma et al., 2022; Yadav et al., 2021). Children and pregnant women are among the most vulnerable groups. The chronic presence of heavy metals in the environment exacerbates these issues, emphasising the critical need for appropriate management and remediation plans (Huang et al., 2022; Brdarić et al., 2021).

The absorption of heavy metals by plants and microorganisms is an important field of research because it determines their bioavailability and entry into the food chain (Priya et al., 2022; Alireza et al., 2021; Bhatt et al., 2020). Understanding heavy metal absorption mechanisms can help inform remediation techniques and sustainable agriculture practices to mitigate their effects (Wang et al., 2021; Cao et al., 2020). Several factors, including soil type, pH, organic matter, and plant species, influence the degree of heavy metal uptake (Pande et al., 2022; Lan et al., 2020).

This study work seeks to investigate the mechanisms underpinning heavy metal absorption, with an emphasis on the physiological and biochemical processes involved. This study aims to provide insights into efficient ways for managing

INTRODUCTION:

Naturally occurring elements with large atomic weights and densities, known as heavy metals, can be harmful at high amounts (Azari et al., 2020; Baragaño et al., 2020). Their widespread presence and harmful consequences on ecosystems, wildlife, and human health have drawn more attention to them than ever before (Sayqal, A. and Ahmed, O. B., 2021; Xu et al., 2020). Heavy metal buildup in soil and water bodies is a result of industrial operations, agricultural methods, and urban runoff (Alotaibi et al., 2021; Briffa et al., 2020). This poses major threats to the environment and public health. They have the potential to disrupt biological processes in ecosystems, resulting in decreased biodiversity and stunted plant and animal growth (Pham et al., 2021). Contaminated soil and water can accumulate these metals, which eventually infiltrate the food chain and impact higher trophic

heavy metal contamination and improving absorption efforts by investigating the interactions between heavy metals and the microbial system. Ultimately, a thorough understanding of heavy metal absorption will help to develop novel strategies for protecting environmental health and supporting sustainable land use.

METHODS:

Bacterial Strain Identification:

The strains in this investigation have been grown on M9 minimum media (M9, 20% glucose, 1 M MgSO₄, and 1 M CaCl₂). Bacterial strains' biochemical characteristics were determined using bergey's manual. Furthermore, the 16S rRNA sequences of the bacterial strains were determined using direct sequencing of the PCR products. DNA extracts from each strain were made using the isolation kit (GeNei). To identify isolates, the full-length 16S rRNA genes were amplified using bacteria-specific primers 27F (5'-AGAGTTTGATCCTGGCTCAG-3') and 1492R (5'-GGTTACCTTGTACGACTT-3') (Nguyen et al., 2013). The purified PCR products were sequenced and Complete 16S rRNA gene sequences were compared using the Basic Local Alignment Search Tool (BLAST) algorithm with other reference sequences that were found in the NCBI database. Phylogenetic trees were created using the neighborjoining approach to compute evolutionary distances (Tamura et al., 2021). MEGA 11 was used to perform neighbour joining analysis. The strains were found to be similar to the 16S rRNA sequences of Klebsiella sp. (strain R2), Klebsiella sp. (strain R19), Serratia sp. (strain L2), and Raoultella sp.

Analysis of minimum inhibitory concentrations to metals:

To evaluate metal resistance (As³⁺, Pb²⁺, Zn²⁺, or Cr⁶⁺), Bowman et al. (2018) used stock solutions of As (NaAsO₂), Cr (K₂Cr₂O₇), Pb (Pb [NO₃]₂), and Zn (ZnSO₄.7H₂O) with distilled water to achieve final concentrations of 1,000 and 10,000 mg L⁻¹, respectively. Metal solutions were sterilised with a 0.2 µm Nalgene vacuum filtration system (Thermo Scientific, Waltham, MA). Polysulfone filters were used to prevent metal sorption on the filter device (Wu et al., 2005). The sensitivity of the strain to four distinct metals was evaluated on a metal-treated M9 minimal medium. Metal modified media were made by adding increasing amounts of metal stock solutions to autoclaved media. For inoculating 96-well plates, add 200 µL of broth medium and 20 µL of mid-logarithmic-phase cultures. The SBT1500 Microplate Shaker (Southwest Science, Hamilton, NJ) was utilised to shake the plates at room temperature while incubating at 150 rpm. Following a 24-hour

incubation period at room temperature in the dark, the metals described in this study had the lowest MICs (minimal inhibitory concentrations) that suppressed bacterial growth. Positive controls included growth media inoculated with metal-free bacterial strains. The strains' growth was monitored using a Sunrise microwell plate reader (Tecan, Research Triangle Park, NC) with an optical density of 595 nm. The plate reader's detection threshold determined whether or not there was any growth.

Bioremediation assay in aqueous solutions:

Bacteria culture (100 mL) were contained in dialysis tubing and pretreated with 0.1 N HCl to remove metal ions that may have been bound to the negatively charged groups of the cell membrane. After 30 minutes of soaking in 0.1 N HCl, the cell cultures were dialysed against deionised water for 24 hours while being stirred continuously at 100 rpm to eliminate residual HCl. Dialysed cultures were placed into 1 L aqueous solutions containing 10 mg L⁻¹ of As³⁺, Pb²⁺, Zn²⁺, and Cr⁶⁺ for 24 hours. This metal concentration (10 mg L⁻¹) is similar to those employed in other dialysis tests to test bacterial cell or EPS binding capability with metals (Bowman et al., 2018). To avoid any possible hydroxide precipitation, the pH of the system was adjusted to 4.5–5.5. The experiment was performed at 37°C.

Optimization for Resistance and Removal Assay:

This study optimised three parameters: carbon supply, nitrogen source, and carbon/nitrogen ratio (C/N). The carbon sources analysed were glucose, maltose, sodium acetate, and sucrose, while the nitrogen sources consisted of potassium nitrate (KNO₃), peptone, yeast extract, and tryptone. The utilised C/N ratios were 5:5, 5:4, 5:3, and 5:2. Optimisation tests were performed separately for each carbon and nitrogen source using the designated C/N ratios in minimal media comprising carbon source (5 g/L), nitrogen source (2 g/L), magnesium sulphate (0.5 g/L), water (1 L), and heavy metal (150 mg/L). This study utilised a neutral pH. Following media preparation and sterilisation, the respective isolates were employed for inoculation and incubated at 35 °C ±2 °C for 96 hours. Following incubation, the growth rates of the isolates and the residual metal concentrations in both inoculation and uninoculated conditions were evaluated to determine the metal tolerance index and the percentage of metal removal.

FT-IR analysis:

Fourier transform infrared spectroscopy was used to identify functional groups in bacterial strains that may be involved in metal uptake during the biosorption process. This approach has been shown

to be useful for delivering structural information on metal cation binding in microorganisms (Gupta et al., 2020). FT-IR analysis was performed on cells before and after metal uptake in an aqueous solution containing eight metals (As^{3+} , Pb^{2+} , Zn^{2+} , and Cr^{6+}) at a concentration of 10 mg/L. Infrared spectra of the control before and after metal uptake were analysed on lyophilised cells using Attenuated Total Reflection (ATR).

Scanning Electron Microscopy-Energy Dispersive Spectroscopy (SEM-EDS):

The pelleted *B. subtilis* cells, post-biosorption, were dried under vacuum, affixed to a suitable stud surface, subsequently gold-sputtered, and examined and photographed using a Scanning Electron Microscope (Zeiss EVO HD 15, Zeiss, Germany) operating at 20.0 kV. The microscope was outfitted with an Inca Penta FETx3 energy dispersive X-ray system (England, UK). To acquire data on the elemental composition of bacterial cell surfaces in metal biosorption studies, the energy dispersive X-ray spectrum for each bacterial isolate was obtained and analysed in relation to individual metal ion solution treatments, revealing the elemental composition of the respective metals on the cell surface (Einhäuser, 1997; Poatak et al., 1980).

Table 1 Procedure of enzymatic activity of alkaline phosphatase

	100 mM Glycine buffer	15.2 mM PNPP solution	Mix by inversion and incubate at 37°C, for exactly 10 minutes	Distill water	Enzyme solution	Mix by inversion and incubate at 37°C, for exactly 10 minutes	20mM NaOH	Mix by inversion	Absorbance at 410nm
BLA NK	0.50 ml	0.50 ml		0.10 ml	-		10 ml		
TES T	0.50 ml	0.50 ml		-	0.10 ml		10 ml		

$$\text{Enzymatic activity} \left(\frac{\text{Units}}{\text{ml}} \right) = \frac{(\text{A410nm Test} - \text{A410nm Blank})(11.1)(df)}{(18.3)(0.1)(10)}$$

Statistical Analysis:

All statistical analyses were carried out using the SPSS statistical software (version 23.0). Comparison of means was determined using the One-Way Analysis of Variance (ANOVA) test, while multiple comparison was determined using the Tukey Multiple Range test. All analyses were carried out at a 95% confidence interval.

RESULT AND DISCUSSION:

Bacterial Identification:

The unknown bacterial culture was identified as *Bacillus cereus* through 16S rRNA sequencing and biochemical characterization was presented in table 1. 16S rRNA gene size was determined as >1500

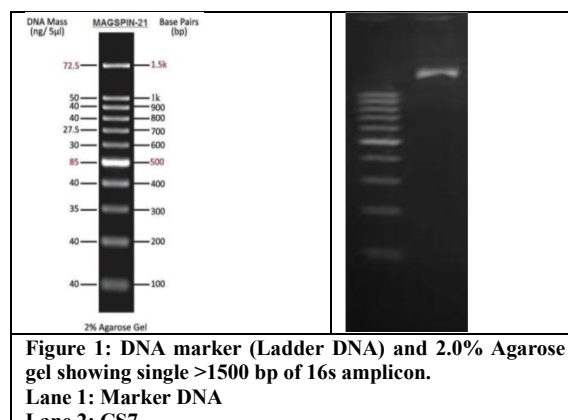
Screening and Production of alkaline phosphatase:

Phosphatase agar media was used for the screening of alkaline phosphatase. Positive results indicated by the appearance of yellow coloration in the media around the streaked microorganism that represent production of alkaline phosphatase enzyme by micro-organism. Negative results indicated by no change in the coloration of media around the bacterial colonies. The production of Alkaline phosphatase enzyme was done by submerged fermentation and the media composition with some modifications as suggested by Nomoto et al., 1988; Prada et al., 1996.

Enzymatic activity of Alkaline phosphatase:

Alkaline phosphatase is a hydrolase enzyme. This enzyme can remove the phosphate groups (phosphorylation) from many types of molecules that includes nucleotides, proteins, and alkaloids. Alkaline phosphatases are most effective in carrying about phosphorylation activity in an alkaline environment and sometimes also called as basic phosphatase (Brent E., 1974). Enzymatic activity of Alkaline phosphatase (AKP) enzyme calculated by following equation.

bp through gel electrophoresis using of the ladder MAGSPIN-21 (Fig.1) and phylogenetic tree was also presented in Fig.2.



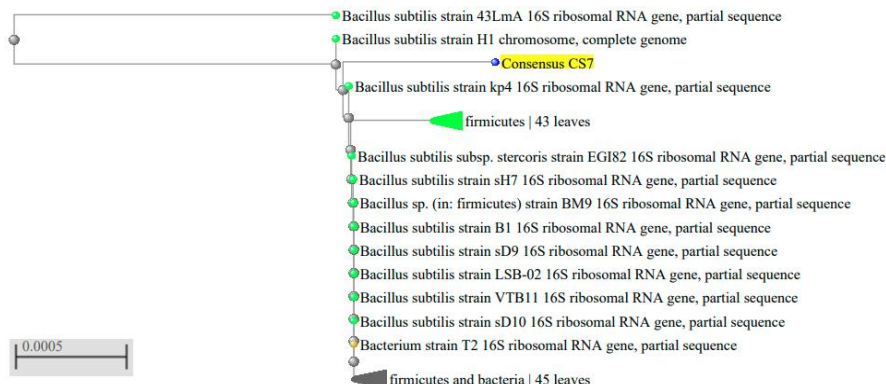


Figure 2: BLAST phylogeny tree

Table 2 Biochemical Characterization of *Bacillus subtilis*.

SN	Test	Result
1.	Indole test	Negative
2.	Methyl red test	Positive
3.	Voges Proskauer test	Positive
4.	Citrate test	Positive
5.	Glucose fermentation test	Positive
6.	Lactose fermentation test	Positive
7.	Maltose fermentation test	Positive
8.	Mannitol fermentation test	Positive
9.	Sucrose fermentation test	Positive
10.	Oxidation fermentation test	Positive
11.	Casein hydrolysis	Positive
12.	Gelatin hydrolysis	Positive
13.	Cellulose test	Positive
14.	Urease test	Positive
15.	Catalase test	Positive
16.	Oxidase test	Positive
17.	Nitrate reduction test	Positive

Tolerance Analysis to Metals:

The minimum inhibitory concentrations (MICs) of the four distinct metals for the corresponding bacterial strain are shown in Table 2. Overall, the strain was more robust against As^{3+} (250–450 mg L $^{-1}$), Pb^{2+} (700–800 g mL $^{-1}$), and Zn^{2+} (500–1,100 mg L $^{-1}$) than against Cr^{6+} (5–10 mg L $^{-1}$). The hierarchy of metal tolerance for the bacterial strain was as follows, it was $\text{Zn}^{2+} > \text{Pb}^{2+} > \text{As}^{3+} > \text{Cr}^{6+}$.

Table 3 Minimum inhibitory concentrations of metals.

Minimum inhibitory concentrations (MIC) (mg L $^{-1}$)	Strain
As	250
Cr	10
Pb	700
Zn	1000

Bioremediation Assay:

The investigation into the metal removal capabilities of the bacterial strain was conducted using individual single-metal solutions, each containing 10 mg L $^{-1}$ of As^{3+} , Pb^{2+} , Zn^{2+} , and Cr^{6+} . The study spanned various time intervals over a 24-h. Over time, the metals were gradually extracted from the solutions, with saturation of the metal

removal capacity achieved within approximately 4 to 5 h. *Bacillus subtilis* (ranging from 4.4 to 318 mg g $^{-1}$ dry mass) The efficiency of metal removal in single-metal solutions was containing all four metal cations. Notably, in single-metal solutions, *Bacillus subtilis* exhibited removal efficiencies of ≥ 150 mg g $^{-1}$ dry mass for Pb^{2+} , and Zn^{2+} and ≤ 150 mg g $^{-1}$ dry mass for As^{3+} , and Cr^{6+} (Figure 3).

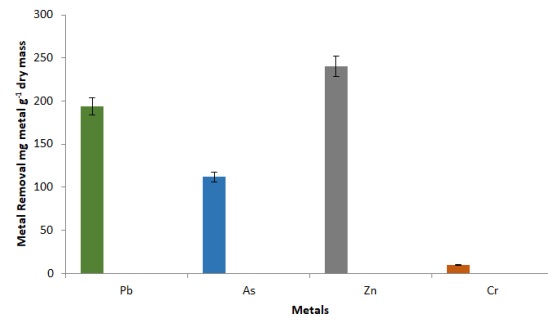


Fig. 3 Metal removal by *Bacillus subtilis*.

Effect of External Carbon Sources:

The highest tolerance index for lead was observed in media containing sodium acetate as the carbon source ($p \leq 0.05$), with the greatest tolerance values recorded in media containing maltose and glucose, respectively. A markedly elevated tolerance index for chromium was noted in media containing sodium acetate. The percentage removal of heavy metals varied from 58.83% (glucose) to 76.33% (sucrose) for lead, from 38.03% (glucose) to 65.27% (sucrose) for chromium, from 71.23% (glucose) to 83.23% (sucrose) for arsenic, and from 69.43% (glucose) to 81.83% (sucrose) for zinc, in the presence of the test bacterial species.

Table 4. Tolerance index to the heavy metals in the presence of the *Bacillus subtilis* at different external carbon sources

Heavy Metal	Carbon Source			
	Acetate	Glucose	Maltose	Sucrose
Lead	0.80±0.01	0.76±0.01	0.51±0.01	0.67±0.00
Arsenic	0.41±0.00	0.25±0.00	0.25±0.01	0.20±0.00
Chromium	0.39±0.00	0.25±0.00	0.28±0.01	0.26±0.00
Zinc	0.72±0.00	0.25±0.00	0.52±0.01	0.56±0.01

Table 5 Heavy metal removal in the presence of the *Bacillus subtilis* at different external carbon sources.

Heavy Metal	Carbon Source			
	Acetate	Glucose	Maltose	Sucrose
Lead	66.60±0.08	58.83±0.12	71.57±0.19	76.33±0.38
Arsenic	80.10±0.22	71.23±0.17	78.20±0.15	83.23±0.18
Chromium	58.90±0.27	38.03±0.19	59.87±0.15	65.27±0.69
Zinc	79.10±0.27	69.43±0.27	75.23±0.12	81.83±0.19

Effect of External Nitrogen Sources:

The highest tolerance index observed in the various nitrogen sources utilised in this experiment was in the media containing peptone, ranging from 0.57 to 1.24. The highest values for chromium ($p\leq 0.05$) were recorded in media containing potassium nitrate (0.52). The minimum and maximum tolerance index values for zinc, 0.52 and 1.32, were recorded in media with tryptone and potassium nitrate, respectively. The highest results for arsenic ($p\leq 0.05$) were obtained in medium containing tryptone (0.60). The removal percentages of heavy metals by *Bacillus subtilis* varied, with values ranging from 55.23% (yeast extract) to 72.00% (tryptone), 53.53% (yeast extract) to 76.81% (peptone), 67.13% (peptone) to 86.33% (tryptone), and 60.40% (potassium nitrate) to 86.23% (peptone) for lead, chromium, arsenic, and zinc, respectively.

Table 6. Tolerance index to the test heavy metals in the presence of the *Bacillus subtilis* at the different external nitrogen sources.

Heavy Metal	Carbon Source			
	KNO ₃	Peptone	Yeast Extract	Tryptone
Lead	0.90±0.02	1.24±0.01	0.57±0.01	0.58±0.00
Arsenic	0.49±0.00	0.55±0.00	0.35±0.01	0.60±0.00
Chromium	0.52±0.01	0.28±0.00	0.20±0.01	0.22±0.00
Zinc	1.32±0.03	0.56±0.00	0.66±0.00	0.52±0.00

Table 7. Heavy metal removal in the presence of the *Bacillus subtilis* at different external nitrogen sources.

Heavy Metal	Carbon Source			
	KNO ₃	Peptone	Yeast Extract	Tryptone
Lead	69.43±0.15	71.27±0.42	55.23±0.23	72.00±0.20
Arsenic	81.22±0.12	67.13±0.16	82.30±0.25	86.33±0.15
Chromium	75.17±0.26	76.81±0.29	53.53±0.08	62.43±0.21
Zinc	60.40±0.41	86.23±0.17	65.52±0.21	80.10±0.25

Effect of Different Carbon/Nitrogen Ratio:

The tolerance indices of *Bacillus subtilis* to various heavy metals at certain carbon/nitrogen (C/N) ratios differed among the metals, likely due to the distinct metabolic capacities of *Bacillus subtilis*, a finding that was consistent across all heavy metals. A markedly elevated tolerance index to arsenic was noted at C/N ratios of 5:2 and 5:4. Notably, the highest tolerance index for lead was recorded at a C/N ratio of 5:2 ($p\leq 0.05$), while for chromium, the highest tolerance index was found at C/N ratios of 5:5 or 5:4 ($p\leq 0.05$). The highest values for zinc removal in the presence of the isolate were seen in a medium with a C/N ratio of 5:3. The elimination of lead in the presence of the isolate demonstrated markedly elevated levels at C/N ratios of 5:5 or 5:4. The most effective chromium removal occurred at C/N ratios of 5:5.

Table 8. Tolerance index to the test heavy metals in the presence of the *Bacillus subtilis* at different carbon/nitrogen (C/N) ratios.

Heavy Metal	Carbon Source			
	5:5	5:4	5:3	5:2
Lead	0.51±0.00	0.81±0.00	0.61±0.00	0.92±0.00
Arsenic	0.45±0.00	0.60±0.00	0.45±0.01	0.63±0.00
Chromium	0.59±0.00	0.54±0.00	0.42±0.00	0.43±0.01
Zinc	0.21±0.00	0.39±0.00	0.50±0.00	0.41±0.01

Table 9. Heavy metal removal in the presence of the *Bacillus subtilis* at different carbon/nitrogen (C/N) ratios.

Heavy Metal	Carbon Source			
	5:5	5:4	5:3	5:2
Lead	80.15±0.21	85.24±0.11	79.13±0.02	70.23±0.12
Arsenic	84.12±0.13	70.23±0.26	84.50±0.12	90.12±0.09
Chromium	75.21±0.14	69.37±0.18	70.27±0.30	65.20±0.14
Zinc	49.20±0.04	50.14±0.07	52.25±0.15	41.20±0.25

FTIR Analysis:

FTIR spectra covering the range of 4,000 to 400 cm⁻¹ were obtained for the bacterial strain both before and after the absorption of four metals. The complex structure of the bacterial cell surface was shown by the varied peaks in the metal-free bacterial strain's FT-IR profiles. Although the *Bacillus subtilis* strains had less IR peaks, common bands were visible in the strains before metal uptake. Functional groups such as amino (N-H, NH₂), alkyne (C≡C), carbonyl (C=O), carboxylic (C-O), hydroxyl (-OH), and phosphate (P=O) groups were represented by these infrared bands. Table 9 lists these bands' assignments as well as the particular functional categories. When exposed to metals, changes in band intensity were observed, along with changes in absorption bands and the appearance of new peaks. As the strain came into contact with the metal surroundings, the number of

infrared bands increased. Functional groups associated with aromatic organics, alkynes ($C \equiv C$), alkanes (C-H), as well as hydroxyl, amine, and aldehyde functional groups, were implicated in the metal-loaded IR spectrum changes. Additionally, the *Bacillus subtilis* metal-loaded strain's spectra showed the emergence of additional peaks that showed the presence of hydroxyl (O-H), alcohol

(R-CHO), amine (P-NH, NH₂), alkanes (C-H), carboxyl (C-C), alkynes ($C \equiv C$), and aromatic compounds. These findings demonstrated the complex changes in bacterial cell surfaces brought about by the absorption of several metals, with notable differences depending on the type of bacterial strain (Fig. 4).

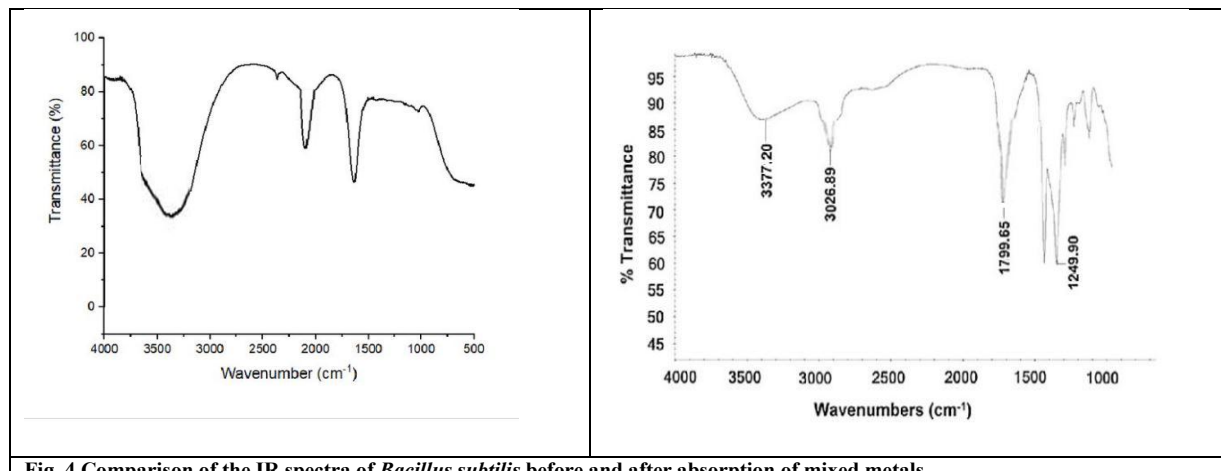


Fig. 4 Comparison of the IR spectra of *Bacillus subtilis* before and after absorption of mixed metals.

Table 10. IR absorption band changes and possible assignment for the metal-free and metal-loaded.

FTIR peak	Metal free	Metal loaded	Displacement	Functional groups	Bond	Assignments
1		684	684	C ₂ H ₂ R ₂	C-H out-of-plane-bend	Alkene
2	720	715	5	1,3-Disubstituted (Aromatic compounds)	C-H out-of-plane-bends	Aromatic
3	741	738	3	1,3-Disubstituted (Aromatic compounds)	C-H out-of-plane-bends	Aromatic
4	810	805	5	C ₂ HR ₃	C-H out-of-plane-bend	Alkene
5		849	849	1,3-Disubstituted (Aromatic compounds)	C-H out-of-plane-bends	Aromatic
6		885	885	1,3-Disubstituted (Aromatic compounds)	C-H out-of-plane-bends	Aromatic
7		1098	1098	(RCO)O	C-O stretch	Carbonyl
8		1118	1118	R-OH	C-O stretches	Alcohol
9		1256	1256	RCOOR'	C-O stretch	Carbonyl
10	1398	1389	9	C-C	C-C bend	Alkane
11	1485	1484	1	P-NH ₂	NH ₂	Amine
12	1523	1513	10	R ₂ C=NR or R ₂ C=NH	C=N stretch	Imine and Oxime
13		1623	1623	R ₂ C=O or RCOOH	C=O stretch	Ketone or carboxylic acid
14	2860	2861	1	C-H	C-H stretch	Alkane
15	3012	3010	2	C=C-H	C-H stretch	Alkene
16	3598	3594	4	RO-H free	O-H stretch	Hydroxyl

Scanning Electron Microscopy-Energy Dispersive Spectroscopy (SEM-EDS) analysis for Surface Biosorption of Heavy Metals

Scanning Electron Microscopy was employed to illustrate the macrostructure of the surface of

desiccated bacterial cell biomass. The Inca Penta FETx3 energy dispersive X-ray system provided clear proof of metal ion attachment to the cell wall of bacterial cells. EDS spectrum scans unequivocally demonstrated that lead, chromium,

arsenic, and zinc ions were adsorbed onto the surface of *B. subtilis* following biosorption. The EDS spectral images, accompanied by the SEM images in the inset, are displayed below.

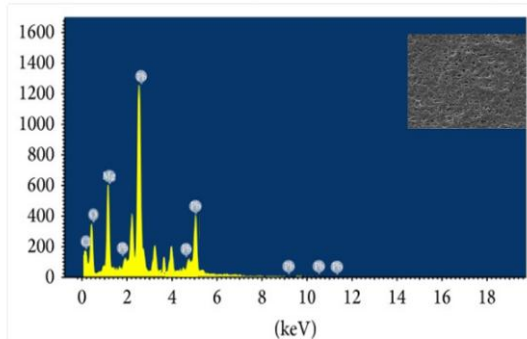


Fig. 5 SEM-EDS analysis of *Bacillus subtilis* metal loaded.

Screening of bacteria for Alkaline phosphatase enzyme production:

The bacteria that are capable for production of alkaline phosphatase enzyme were first screened by Phosphatase agar media that contains p-nitrophenol phosphate (colorless) as the substrate. The bacteria that produce Alkaline Phosphatase enzyme, removes phosphate group from substrate p-nitrophenol phosphate (colorless) to p-nitrophenolate (yellow color) that turns the color of the media to yellow color. In the screening process, *Bacillus subtilis* had shown positive for phosphatase activity indication the production of yellow coloration in the media.



Fig 6: Screening for production of Alkaline phosphatase enzyme by Phosphatase agar media.

Enzymatic activity and Protein fold of Alkaline phosphatase enzyme

The enzymatic activity is used to determine the rate of an enzyme capable for breakdown of substrate or generation of product. The determination of enzyme rate is carried by continuous assay or discontinuous assay. In Continuous assays assay gives a continuous reading of activity, whereas in discontinuous assays, the sample mixture is taken at time intervals or the reaction are stopped and the concentration of substrates/products were determined. The enzyme activity of Crude extract was 36.214 U/ml. In case of purified sample salt precipitation and dialysis sample the enzyme activity was 38.169 U/ml and 35.121 U/ml respectively. The ion exchange sample had 25.257 U/ml of enzyme activity (Table 10).

Table 11 Determination of Specific activity and protein fold for different samples of enzyme.

SAMPLE	Enzyme activity (Units/ml)	Protein content (mg/ml)	Specific activity (U/mg)	Protein fold
Crude	36.214	0.270	138.27	1.00
Salt Precipitation	38.169	0.161	243.28	1.75
Dialysis	35.121	0.147	245.63	1.78
Ion Exchange_Elute 4	25.257	0.080	290.71	2.10

CONCLUSION:

Bacillus subtilis is a good option for the bioremediation of settings affected by heavy metals due to its remarkable metal tolerance and biosorption capabilities. The study demonstrates how the bacterium may adsorb metals including lead, cadmium, and chromium by using exopolysaccharides and its cell wall. Its practical potential is further shown by improved biosorption efficiency under ideal environmental conditions. These results highlight the use of *B. subtilis* as an economical and environmentally beneficial method of treating industrial wastewater and cleaning up the environment. In order to increase its biosorption capacity and broaden its use in various remediation scenarios, future research could concentrate on genetic and metabolic engineering.

REFERENCE:

18. Azari, A., Nabizadeh, R., Nasseri, S., Mahvi, A.H., Mesdaghinia, A.R. (2020). Comprehensive systematic review and meta-analysis of dyes adsorption by carbonbased adsorbent materials: classification and analysis of last decade studies. *Chemosphere* 250, 126238. <https://doi.org/10.1016/j.chemosphere.2020.126238>
19. Alotaibi, B.S., Khan, M., Shamim, S. (2021) Unraveling the underlying heavy metal detoxification mechanisms of *Bacillus* species. *Microorganisms* 2021, 9, 1628.
20. Alireza, F., Nazanin, K., Stephen, J., Coupe, Alan, P., Newman, (2021) A meta-analysis of metal biosorption by suspended bacteria from three phyla, *Chemosphere*, Volume 268, 2021, 129290, <https://doi.org/10.1016/j.chemosphere.2020.129290>.
21. Baragaño, D., Forján, R., Welte, L., Gallego, J. L. R. (2020). Nanoremediation of As and metals polluted soils by means of graphene oxide nanoparticles. *Sci. Rep.* 10:1896. doi: 10.1038/s41598-020-58852-4
22. Bernt, E. (1974) in *Methods of Enzymatic Analysis* (Bergmeyer, H.U., ed) 2nd ed., Volume II, pp 868-870,

Academic Press, Inc., New York, NY

23. Bowman, N., Patel, P., Xu, W., Alsaffar, A., Tiquia-Arashiro, S. M. (2018). Enrichment and isolation of Pb-resistant bacteria from Saint Clair River sediments and their potential for Pb removal in aqueous solutions. *Appl. Microbiol. Biotechnol.* 102, 2391–2398. doi: 10.1007/s00253-018-8772-4

24. Brdarić, E., Soković, Bajić, S., Đokić, J., Đurđić, S., Ruas-Madiedo, P., Stevanović, M., Tolinački, M., Dinić, M., Mutić, J., Golić, N. (2021) Protective Effect of an exopolysaccharide produced by Lactiplantibacillus plantarum BGAN8 against Cadmiuminduced toxicity in Caco-2 Cells. *Front. Microbiol.* 2021, 12, 759378

25. Bhatt, P., Bhatt, K., Huang, Y., Lin, Z., Chen, S. (2020a). Esterase is a powerful tool for the biodegradation of pyrethroid insecticides. *Chemosphere* 244:125507. doi: 10.1016/J.CHEMOSPHERE.2019.125507

26. Briffa, J., Sinagra, E., and Blundell, R. (2020). Heavy metal pollution in the environment and their toxicological effects on humans. *Heliyon* 6:e04691. doi: 10.1016/j.heliyon.2020.e04691

27. Cao, X., Alabresm, A., Chen, Y. P., Decho, A. W., Lead, J. (2020). Improved metal remediation using a combined bacterial and nanoscience approach. *Sci. Total Environ.* 704:135378. doi: 10.1016/j.scitotenv.2019.135378

28. Einhäuser, T. J. (1997) ICP-OES and SEM-EDX analysis of dust and powder produced by the laser-processing of a Cr-Ni-steel alloy. *Mikrochimica Acta* ;127(3):265–268. doi: 10.1007/bf01242733

29. Gupta, A.D., Kavitha, E., Singh, S., Karthikeyan, S. (2020). Toxicity mechanism of Cu²⁺ ion individually and in combination with Zn²⁺ ion in characterizing the molecular changes of *Staphylococcus aureus* studied using FTIR coupled with chemometric analysis. *J. Biol. Phys.* 46, 395–414. doi: 10.1007/s10867-020-09560-7

30. Huang, L., Jin, Y., Zhou, D., Liu, L., Huang, S., Zhao, Y. (2022). A review of the role of extracellular polymeric substances (EPS) in wastewater treatment systems. *Int. J. Environ. Res. Public Health* 19:12191. doi: 10.3390/ijerph191912191

31. Lan, M. M., Liu, C., Liu, S. J., Qiu, R.L., Tang, Y. T. (2020). Phytostabilization of cd and Pb in highly polluted farmland soils using ramie and amendments. *Int. J. Environ. Res. Public Health* 17:1661. doi: 10.3390/ijerph17051661

32. Ma, Y., Bantec, T.N., Oliveira, R.S., Coutinho, A., Zhang, C., Freitas, H. (2022). “The role of bacteria in metal bioaccumulation and biosorption” in *Advances in microbe-assisted phytoremediation of polluted sites*. eds. K. Bauddh and Y. Ma (New York, USA: Elsevier), 103–112.

33. Nguyen, S., Ala, F., Cardwell, C., Cai, D., McKindles, K.M., Lotvol, A. (2013). Isolation and screening of carboxydotrophs isolated from composts and their potential for butanol synthesis. *Environ. Technol.* 34, 1995–2007. doi: 10.1080/09593330.2013.795987

34. Nomoto, M., Ohsawa, M., Wang, C.C.C. and Yeh, K.W. (1988). Purification and characterization of extracellular alkaline phosphatase from an Alkalophilic Bacterium. *AgricBiol Chem.* 52: 1643-1647

35. Pande, V., Pandey, S.C., Sati, D., Bhatt, P., Samant, M. (2022) Microbial Interventions in Bioremediation of Heavy Metal Contaminants in Agroecosystem. *Front. Microbiol.* 13:824084. doi: 10.3389/fmicb.2022.824084

36. Prada, P.D., Curtze, J.L. and Brenchley, J.E. (1996). Production of two extracellular alkaline phosphatases by a Psychrophilic Arthrobacter Strain. *Appl. and EnvirMicrobiol.* 62:3732- 3738

37. Priya, A.K., Gnanasekaran, L., Dutta, K., Rajendran, S., Balakrishnan, D., Soto-Moscoso, M. (2022). Biosorption of heavy metals by microorganisms: evaluation of different underlying mechanisms. *Chemosphere* 307:135957. doi: 10.1016/j.chemosphere.2022.135957

38. Pham, V.H.T., Kim, J., Chang, S., Chung, W. (2021) Investigation of lipolytic-secreting bacteria from an artificially polluted soil using a modified culture method and optimization of their lipase production. *Microorganism*, 9, 2590

39. Pagliaccia, B., Carretti, E., Severi, M., Berti, D., Lubello, C., Lotti, T. (2022). Heavy metal biosorption by extracellular polymeric substances (EPS) recovered from anammox granular sludge. *J. Haz. Mat.* 424:126661. doi: 10.1016/j.jhazmat.2021.126661

40. Pham, V.H.T., Kim, J., Chang, S., Chung, W. (2022) Bacterial Biosorbents, an Efficient Heavy Metals Green Clean-Up Strategy: Prospects, Challenges, and Opportunities. *Microorganisms* 2022, 10, 610. <https://doi.org/10.3390/microorganisms10030610>

41. Postek, M.T., Howard, K.S., Johnson, A.H., McMichael, K.L. (1980). *Scanning Electron Microscopy: A Student's Handbook*. Burlington, Mass, USA: Ladd Research Industries.

42. Sayqal, A., and Ahmed, O.B. (2021). Advances in heavy metal bioremediation: an overview. *Appl. Bionics Biomech.* 2021:1609149. doi: 10.1155/2021/1609149

43. Tamura, K., Stecher, G., and Kumar, S. (2021). MEGA11: molecular evolutionary genetics analysis. *Mol. Biol. Evol.* 38, 3022–3027. doi: 10.1093/molbev/msab120

44. Wang, G., Zhang, Q., Du, W., Ai, F., Yin, Y., Ji, R. (2021). Microbial communities in the rhizosphere of different willow genotypes affect phytoremediation potential in Cd contaminated soil. *Sci. Total Environ.* 769:145224. doi: 10.1016/j.scitotenv.2021.145224

45. Wu, W., Gu, B., Fields, M.W., Gentile, M., Ku, Y.K., Yan, H. (2005). Uranium (VI) reduction by denitrifying biomass. *Biorem. J.* 9, 49–61. doi: 10.1080/10889860590929628

46. Yadav, M.M., Singh, G., Jadeja, R.N. (2021) Physical and chemical methods for heavy metal removal. *Pollut. Water Manag. Resour. Strateg. Scarcity*, 377–397

47. Xu, S., Xing, Y., Liu, S., Hao, X., Chen, W., Huang, Q. (2020). Characterization of Cd²⁺ biosorption by *Pseudomonas* sp. strain 375, a novel biosorbent isolated from soil polluted with heavy metals in Southern China. *Chemosphere* 240, 124893. <https://doi.org/10.1016/j.chemosphere.2019.124893>.